Substrate and Inhibitor Binding Sites in *Corynebacterium glutamicum* Diaminopimelate Dehydrogenase[†,‡]

Giovanna Scapin,*[,§,||] Maurizio Cirilli,[§,⊥] Sreelatha G. Reddy,[§,||] Yong Gao,[#] John C. Vederas,[#] and John S. Blanchard[§]

Biochemistry Department, Albert Einstein College of Medicine, 1300 Morris Park Avenue, Bronx, New York 10469, Istituto di Strutturistica Chimica, CNR, Area della Ricerca di Roma, Monterotondo, Roma, Italy, and Department of Chemistry, University of Alberta, Edmonton, Alberta, Canada

Received November 13, 1997; Revised Manuscript Received January 6, 1998

ABSTRACT: The three-dimensional structures of *Corynebacterium glutamicum* diaminopimelate dehydrogenase as a binary complex with the substrate *meso*-diaminopimelate (*meso*-DAP) and a ternary complex with $NADP^+$ and an isoxazoline inhibitor [Abbot, S. D., Lane-Bell, P., Kanwar, P. S. S., and Vederas, J. C. (1994) *J. Am. Chem. Soc. 116*, 6513−6520] have been solved and refined against X-ray diffraction data to 2.2 Å. Diaminopimelate dehydrogenase is a homodimer of approximately 35 000 molecular weight subunits and is the only dehydrogenase present in the bacterial diaminopimelate/lysine biosynthetic pathway. Inhibitors of the enzymes of L-lysine biosynthesis have been proposed as potential antibiotics or herbicides, since mammals lack this metabolic pathway. Diaminopimelate dehydrogenase catalyzes the unique, reversible, pyridine dinucleotide-dependent oxidative deamination of the D-amino acid stereocenter of *meso*-diaminopimelate to generate L-2-amino-6-oxopimelate. The enzyme is absolutely specific for the *meso* stereoisomer of DAP and must distinguish between two opposite chiral amino acid centers on the same symmetric substrate. The determination of the three-dimensional structure of the enzyme−*meso*-diaminopimelate complex allows a description of the molecular basis of this stereospecific discrimination. The substrate is bound in an elongated cavity, in which the distribution of residues that act as hydrogen bond donors or acceptors defines a single orientation in which the substrate may bind in order to position the D-amino acid center of *meso*-DAP near the oxidized nucleotide. The previously described isoxazoline inhibitor binds at the same site as DAP but has its L-amino acid center positioned where the D-amino acid center of *meso*-DAP would normally be located, thereby generating a nonproductive inhibitor complex. The relative positions of the N-terminal dinucleotide and C-terminal substrate-binding domains in the diaminopimelate dehydrogenase−$NADP^+$, diaminopimelate dehydrogenase−DAP, and diaminopimelate dehydrogenase−$NADP^+$−inhibitor complexes confirm our previous observations that the enzyme undergoes significant conformational changes upon binding of both dinucleotide and substrate.

meso-Diaminopimelate (*meso*-DAP) and lysine are synthesized in bacteria in eight and nine steps, respectively, from aspartate (*1*, *2*). The first two steps in the synthesis, the conversion of aspartate to aspartyl phosphate and the reduction of aspartyl phosphate to aspartate semialdehyde, are shared with the threonine and methionine biosynthetic pathways. Dihydrodipicolinate synthase, encoded by the *dap*A gene, and dihydrodipicolinate reductase, encoded by the *dap*B gene, catalyze the third and fourth step in the pathway, respectively, and are the enzymes which commit flux to the biosynthesis of DAP and lysine and are common to all bacterial species (Scheme 1). The synthesis of DAP from L-tetrahydrodipicolinate, the product of the reductase, can be accomplished by three separate routes: the succinylase (*3*, *4*) and acetylase pathways (*5*), in which N-succinylated or N-acetylated intermediates are generated, and the infrequently encountered dehydrogenase pathway (*6*). Most bacteria utilize only one of the three routes, and the succinylase pathway is used by all Gram-negative and many Gram-positive species, whereas the acetylase pathway is limited to certain *Bacillus* species. Diaminopimelate dehydrogenase, the enzyme which directly converts tetrahydrodipicolinate to *meso*-diaminopimelate, has only been identified in *Bacillus* species, *Brevibacterium* species, and *Corynebacterium glutamicum* (*7*, *8*). In *C. glutamicum*, the dehydrogenase and succinylase pathways have been shown to operate simultaneously (*9*). These authors have suggested that while the dehydrogenase pathway may be not essential, the additional biosynthetic capacity provided by the dehydrogenase may allow for increased synthesis of *meso*-DAP and L-lysine. In *C. glutamicum*, 30% of the lysine produced by the bacterium is generated via the dehydrogenase, with the remainder being generated using the succinylase pathway enzymes (*10*). Mammals lack the capacity to synthesize L-lysine and require this amino acid in their diet, suggesting

[†] This work was supported by NIH Grant AI33696, the Natural Sciences and Engineering Research Council (NSERC) of Canada, and Merck Frosst Canada.

[‡] The coordinates have been deposited with the Brookhaven Protein Data Bank, PDB codes 2DAP and 3DAP.

* To whom correspondence should be addressed: (732) 594-8429; fax (732) 594-5042.

[§] Albert Einstein College of Medicine.

[||] Current address: Merck Research Laboratories, P.O. Box 2000, RY50-105, Rahway, NJ 07065.

[⊥] Istituto di Strutturistica Chimica, CNR.

[#] University of Alberta.

S0006-2960(97)02794-3 CCC: $15.00 © 1998 American Chemical Society
Published on Web 02/18/1998

Scheme 1

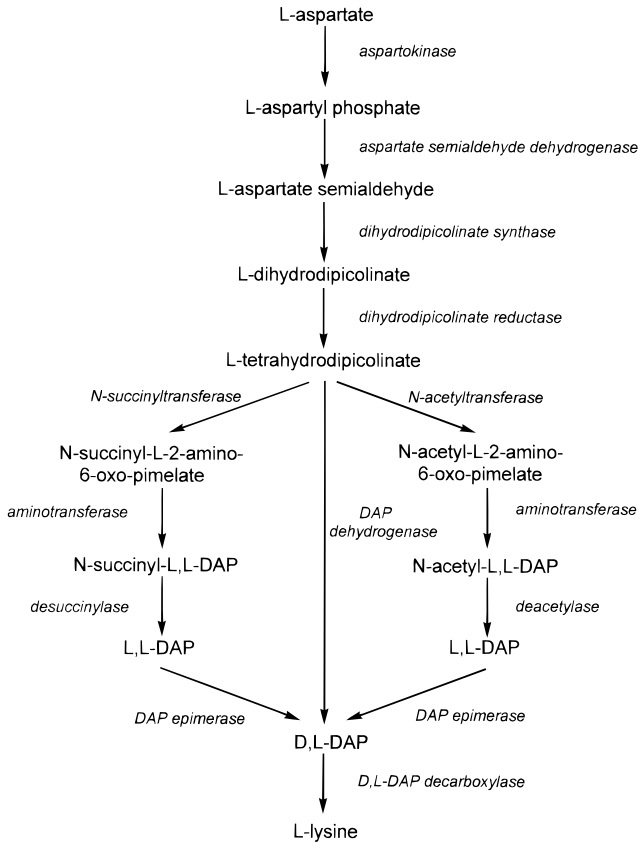

Scheme 2: Reaction Catalyzed by Diaminopimelate Dehydrogenase

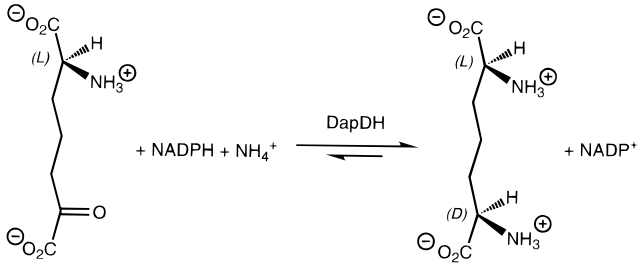

that inhibitors of bacterial L-lysine biosynthesis may be effective, nontoxic antimicrobial compounds.

The NADPH-dependent diaminopimelic acid dehydrogenase (DapDH; EC 1.4.1.16) catalyzes the direct conversion of the acyclic form of L-tetrahydrodipicolinate, L-2-amino-6-oxopimelate, into *meso*-DAP (Scheme 2). The dehydrogenase belongs to a group of pyridine dinucleotide-dependent enzymes that catalyze the oxidative deamination of an amino acid to its corresponding keto acid and ammonia (*11*). DAP dehydrogenase is very unusual in that it is the only amino acid dehydrogenase which stereospecifically oxidizes a D stereocenter. The enzyme is absolutely specific for the *meso* form of the substrate and thus must be able to distinguish between the two chemically identical, but stereochemically opposite, centers on the same symmetric molecule. The enzyme has been isolated, purified, and enzymatically characterized from *Bacillus sphaericus* and *Brevibacterium* species (*7*, *12*). The equilibrium constant was determined to be 4.5×10^{-14} M^2 at pH 7.3, making diaminopimelate synthesis thermodynamically favorable. Although no detailed investigation of the mechanism has been performed, by analogy with other amino acid dehydrogenases, it has been assumed that the reaction may proceed through an imine intermediate, generated by reaction of ammonia with the keto acid (*13*). This information has been used as a starting point for designing conformationally restricted analogues, which are sp^2-hybridized at positions equivalent to the α-D stereocenter and act as inhibitors of the enzyme.

The *ddh* gene encoding the *C. glutamicum* diaminopimelic acid dehydrogenase has been sequenced (*14*), and the 320-residue enzyme has been expressed at high levels in *Escherichia coli* (*15*). The three-dimensional structure of the binary complex enzyme−NADP$^+$ has been solved and refined to 2.2 Å resolution (*16*). This structure identified the molecular basis for NADP$^+$ specificity, suggested a likely substrate binding site, and implied that a significant conformational change was required after substrate binding but before catalysis. To probe the structural basis for the stereochemical discrimination required by the enzyme, in the present work the structure of the binary enzyme−DAP has been solved and refined against 2.2 Å X-ray diffraction data. In addition, the structure of the ternary complex formed from the enzyme, NADP$^+$, and (2*S*,5*S*)-2-amino-3-(3-carboxy-2-isoxazolin-5-yl)propanoic acid, an inhibitor of the dehydrogenase (*13*), has been solved and refined to 2.2 Å resolution.

EXPERIMENTAL PROCEDURES

Crystallization and Data Collection. Recombinant *C. glutamicum* diaminopimelate dehydrogenase was purified as previously described (*15*). Crystals of the binary diaminopimelate dehydrogenase−DAP complex were obtained using the hanging drop vapor diffusion method, with 12−14% PEG 8000 as precipitant, in 150−300 mM magnesium acetate and 100 mM sodium cacodylate, pH 6.5. Crystals were grown at room temperature from 6 μL drops which contained 3 μL of protein solution (20 mg/mL protein containing 2 mM NADP$^+$ and 30 mM DAP) and 3 μL of precipitant solution. Crystals in the shape of elongated, thick needles appeared between 3 and 5 days and reached their maximum dimensions in about 2 weeks. A typical crystal measured approximately 0.04 × 0.04 × 0.5 mm and diffracted to about 2.2 Å. An initial diffraction data set to 2.5 Å was collected at 16 °C using a Rigaku RU-200 rotating anode X-ray source operating at 55 kV and 85 mA and a Siemens multiwire area detector. The unit cell parameters were $a = b = 121.4$ Å, $c = 52.3$ Å, $\alpha = \beta = 90.0°$, and $\gamma = 120.0°$. Data were integrated in a low-symmetry space group (i.e., assuming *P*3 symmetry) so as not to remove any reflections in the reduction step. Data processing, scaling, and merging were done using the XENGEN software package (*17*). Analysis of the integrated data set showed that the pattern of reflections was consistent with trigonal crystals, space group *P*321. The calculated unit cell volume was 672 890 Å^3. The monomeric molecular weight of *C. glutamicum* diaminopimelate dehydrogenase is 35 200, and assuming one molecule per asymmetric unit, we obtained a V_m ratio (volume/protein molecular mass) of 3.2 Å^3/Da, corresponding to a solvent content of about 60%. These values fall within the range expected for globular proteins (*18*). A 94.8% complete data set to 2.2 Å was collected from a second crystal and used for the structure solution and refinement.

Table 1: Statistics for Crystals Used for the Three-Dimensional Structure Determination of the Binary Complex Diaminopimelate Dehydrogenase−DAP and the Ternary Complex Diaminopimelate Dehydrogenase−$NADP^+$−Isoxazoline[a]

	DapDH−DAP	DapDH−$NADP^+$−inhibitor
space group	trigonal, *P*321	monoclinic, $P2_1$
unit cell parameters	$a = b = 121.4$ Å, $c = 52.3$ Å; $\alpha = \beta = 90°$, $\gamma = 120°$	$a = 75.6$ Å, $b = 65.6$ Å, $c = 84.5$ Å; $\beta = 106.5°$
molecules/au	1	2
resolution range (Å)	10−2.2	19.0−2.0
no. of observations	86282 (7642)	70458 (5440)
no. of reflections	21456 (2297)	46303 (4342)
completeness (%)	94.8 (82.3)	88.9 (77.7)
$I/\sigma I$	10.7 (2.1)	10.0 (2.5)
$R_{sym}(I)$	10.2 (29.3)	7.4 (20.9)

[a] Numbers in parentheses represent measurements in the last shell of resolution (2.3−2.2 Å for the DapDH−DAP Complex and 2.1−2.0 Å for the DapDH−$NADP^+$−inhibitor complex).

Crystals of the ternary diaminopimelate dehydrogenase−$NADP^+$−(2*S*,5*S*)-isoxazoline complex were obtained under the same conditions described above, after preincubation of the protein (15 mg/mL) with 2 mM $NADP^+$ and 0.75 mM inhibitor at 4 °C for 2 h. The (2*R*,5*R*)- and (2*R*,5*S*)-isoxazoline isomers were prepared analogously to the corresponding 2*S* isomers (*13*). These crystals were completely isomorphous with the crystals used in the initial diaminopimelate dehydrogenase−$NADP^+$ structure determination (*16*): monoclinic, space group $P2_1$, with $a = 75.6$ Å, $b = 65.6$ Å, $c = 84.5$ Å, and $\beta = 106.5°$. There were two molecules per asymmetric unit, corresponding to a solvent content of about 55%, and these crystals diffracted to 2.0 Å. An 89% complete data set to 2.0 Å was collected at 16 °C using the same Rigaku RU-200 rotating anode X-ray source operating at 55 kV and 85 mA and a Siemens multiwire area detector. Table 1 summarizes the data collection statistics.

Structure Solution and Refinement. The three-dimensional structure of the binary *C. glutamicum* diaminopimelate dehydrogenase−DAP complex was solved by molecular replacement techniques, using as a search model the open monomer of the diaminopimelate dehydrogenase−$NADP^+$ complex refined to 2.2 Å (*16*) without bound nucleotide or water molecules. The rotation function was calculated with AMORE (*19*), using 10.0−4.5 Å data, and gave a single solution with a correlation coefficient of 13.3 (the next best solution had a correlation coefficient of 10.0). The translation function was calculated with this rotation function solution and 9.0−4.5 Å data and gave a single solution with a correlation coefficient of 39.9 and *R*-factor of 45.8%. The solution was subjected to 50 cycles of rigid body refinement as implemented in X-PLOR (*20*) using data between 8 and 3.5 Å (5237 reflections with $F > 2\sigma F$, 98% of possible). The *R*-factor went from 48.0% to 44.7%. Ten percent of the reflections were set aside for *R*-free calculation (*21*, *22*), and the model was subjected to a 3000° simulated annealing refinement as implemented in X-PLOR, using data between 8.0 and 2.8 Å (13 048 reflections with $F > 2\sigma F$, 97.0% of possible). The *R*-factor and *R*-free were 24.9% and 36.4%, respectively, and the model maintained good geometry (rmsd for bond lengths and bond angles were 0.015 Å and 2.0°, respectively). Inspection of a difference Fourier electron density map clearly showed electron density corresponding to bound DAP, but there was no evidence for bound cofactor. Refinement of the *C. glutamicum* diaminopimelate dehydrogenase−DAP binary complex was continued by alternate cycles of manual rebuilding of the model and computer-based refinement. The simulated annealing and least-squares minimizations, and the individual *B*-factor refinement implemented in the X-PLOR suite of programs, were performed throughout the refinement. "Shake omit" electron density maps (maps calculated by omitting portions of the chain from the model and applying to the remaining atoms a random error to the *x*, *y*, *z* coordinates before calculating the maps) were extensively used to check and rebuild several regions of the model, including residues 55−72, 186−218, and 305−310, and the side chains of several residues. The resolution was gradually increased to include all available data in the range 8.0−2.4 Å (16 389 reflections with $F > 2\sigma F$, 95.5% of possible). The progress of the refinement was always monitored using cross-validation methods, and only those operations that resulted in a lower *R*-free were used in the refinement. Several rounds of refinements were necessary to lower the crystallographic *R*-factor to 22.3% (*R*-free was 33.0%). With this model, a molecule of DAP was built into the available electron density. In the next round of refinement, two solvent molecules, one of which is located on the crystallographic 3-fold axis and one on the crystallographic 2-fold axis, were also built into the model, and the resolution was further extended to include data to 2.2 Å. In the last steps of the refinement, extensive geometry checks were run using WHAT_IF, and the model was corrected accordingly. The final model contains one diaminopimelate dehydrogenase monomer, one DAP molecule, and 150 solvent molecules per asymmetric unit. The crystallographic *R*-factor for 20 794 reflections between 10.0 and 2.2 Å with $F > 2\sigma F$ (91.9% of possible) is 19.2% (*R*-free is 25.8%), with root-mean-square deviations in bond lengths and bond angles of 0.011 Å and 1.7°, respectively. Table 2 summarizes statistics on the final model.

Table 2: Statistics for Refined Models of Diaminopimelate Dehydrogenase−DAP and Diaminopimelate Dehydrogenase−$NADP^+$−Inhibitor Complexes

	DapDH−DAP	DapDH−$NADP^+$−inhibitor
no. of reflections ($F > 2\sigma F$)	20794	34783
resolution range (Å)	10.0−2.2	19.0−2.2
R-factor (%)[a]	19.2 (19.5)	17.5 (17.9)
free *R*-factor (%)[a]	25.8 (26.2)	23.3 (23.7)
rms bond lengths (Å)	0.011	0.009
rms bond angles (deg)	1.7	1.5
protein atoms	2445	4928
solvent atoms	150	133
ligand atoms	13	110

[a] Numbers in parentheses are the values for all reflections (no σ cutoff).

Since crystals of the diaminopimelate dehydrogenase−$NADP^+$−inhibitor complex were isomorphous with the original diaminopimelate dehydrogenase−$NADP^+$ crystals, molecular replacement was not required to solve the structure. The bound dinucleotide and the inhibitor were clearly visible in a $((|F_o| - |F_c|)\Phi_c)$ difference Fourier electron density map, calculated using the F_o from the ternary complex and F_c and phases from the protein model (two

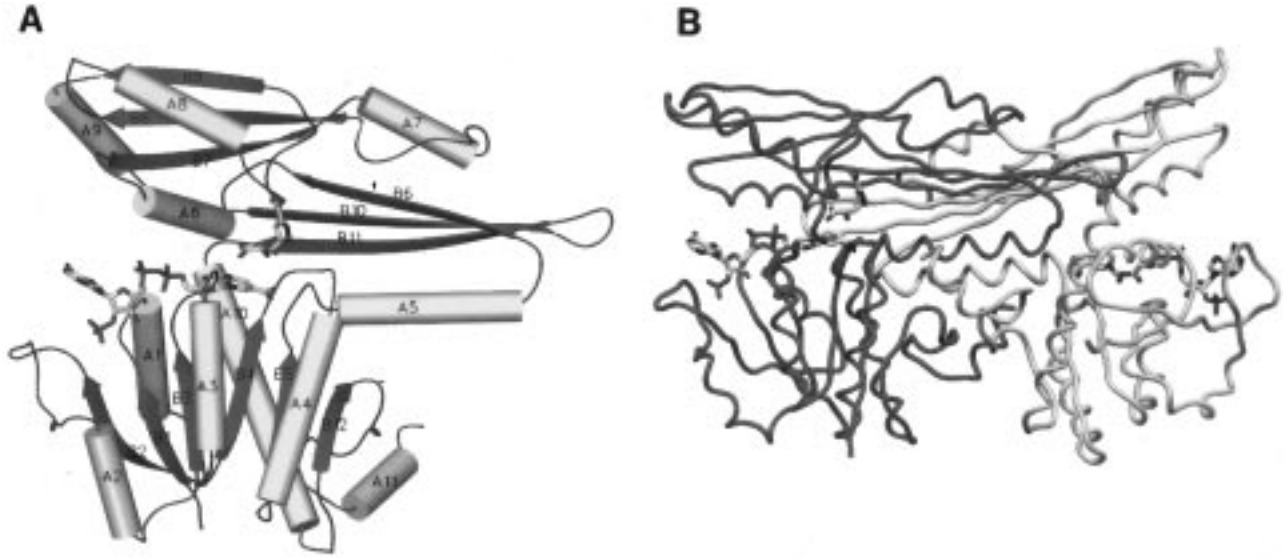

FIGURE 1: (A) Ribbon diagram of the *C. glutamicum* diaminopimelate dehydrogenase monomer. The bound dinucleotide and inhibitor are also displayed. (B) Ribbon diagram of the *C. glutamicum* diaminopimelate dehydrogenase dimer.

monomers, without ligands and solvent molecules). The refinement of this complex was carried out in a manner similar to that previously described for the binary complex, alternating cycles of manual rebuilding of the model and computer-based refinement. The final model contains one diaminopimelate dehydrogenase dimer, two molecules of $NADP^+$, one molecule of inhibitor, and 133 water molecules per asymmetric unit. The crystallographic *R*-factor for 34 783 reflections between 19.0 and 2.2 Å with $F > 2\sigma F$ (86.0% of possible) is 17.5% (*R*-free is 23.3%), with root-mean-square deviations in bond lengths and bond angles of 0.009 Å and 1.5°, respectively. Table 2 summarizes statistics on the final model.

RESULTS AND DISCUSSION

The structures of the binary complex between *C. glutamicum* diaminopimelate dehydrogenase and the substrate *meso*-diaminopimelic acid (DAP) and of the ternary complex between diaminopimelate dehydrogenase, $NADP^+$, and the inhibitor (2*S*,5*S*)-2-amino-3-(3-carboxy-2-isoxazolin-5-yl)-propanoic acid [(2*S*,5*S*)-isoxazoline; *13*] have been solved and refined against 2.2 Å X-ray diffraction data. The binary complex crystallized in a trigonal space group, with one molecule per asymmetric unit. The enzyme is known to exist as a homodimer in solution (*15*, *16*), and in this space group a dimer is generated by a crystallographic 2-fold axis. The ternary complex crystallized in a monoclinic space group, identical to that previously reported for the enzyme−$NADP^+$ complex, with one dimer per asymmetric unit. Figure 1A shows a ribbon diagram of the diaminopimelate dehydrogenase monomer, and Figure 1B is a ribbon diagram of the dimer. Both the binary enzyme−DAP and ternary complexes have been refined to reasonable *R*-factors (19.2% and 17.5%, respectively, with *R*-free of 25.8% and 23.3%), and the models retained excellent geometry (Table 2), with ϕ, ψ angles that fall within the allowed region of low energy in the Ramachandran plot.

The fold of diaminopimelate dehydrogenase has been previously described (*16*) and will only briefly be described here. The enzyme is composed of three domains: a dinucleotide binding domain, spanning residues 1−118 and 269−299, containing five α-helices (A1−A4 and A10 in Figure 1A) and six parallel β-strands (B1−B5 and B12 in Figure 1A); a dimerization domain, composed of residues 122−145, 244−267, and 300−320, that form three long, antiparallel β-strands and one α-helix (B6, B10, and B11 and A5 in Figure 1A); and a third domain, spanning residues 150−239, that has been proposed to be the substrate-binding domain (*16*) and contains three antiparallel β-strands (B7−B9 in Figure 1A) and four α-helices (A6−A9 in Figure 1A). Residues of helix A5 are involved in dimer formation and have been shown to be highly protected from hydrogen/deuterium exchange in electrospray mass spectrometry studies (*23*). Analysis of the protein backbone of the two complexes shows that while the structures of the three domains are very similar, their relative positions are different. The presence of an asymmetric dimer in the asymmetric unit of the monoclinic space group has already been described and imputed to be due to the presence of two molecules of acetate in one of the presumptive *meso*-diaminopimelate binding sites (*16*). Figure 2A is an overlay of the Cα traces for the two subunits of the asymmetric dimer in the monoclinic space group, demonstrating the presence of a rigid body movement of the two domains accompanying amino acid substrate binding. On the basis of this crystallographic evidence, and by analogy to previous studies of glutamate dehydrogenase (*24*−*26*), the two monomers have been described as existing in an "open", or "binding", conformation (yellow monomer) and in a "closed", or "active", conformation (magenta monomer). Figure 2B shows an overlay of the Cα trace for the two monomers of the monoclinic space group, one of which contains $NADP^+$ but no DAP, and the monomer from the asymmetric unit of the trigonal space group, which contains DAP but no $NADP^+$ (blue). The relative position of the dinucleotide-binding/dimerization domains, and the amino acid-binding domain in the enzyme−DAP binary complex, is different from either the open or closed conformations previously observed and corresponds to an intermediate conformation. Analysis of the molecular surfaces performed using GRASP (*27*) shows

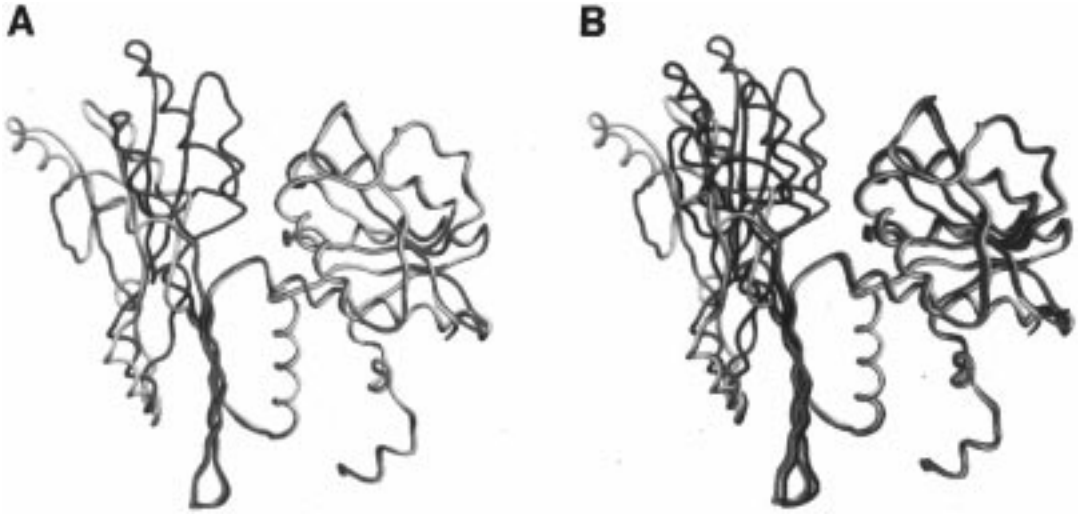

FIGURE 2: (A) Overlay of the Cα trace of the two monomers in the diaminopimelate dehydrogenase dimer, as found in the monoclinic space group asymmetric unit (ternary complex). The open monomer is in yellow, and the closed monomer is in magenta. (B) Overlay of the Cα trace of the two monomers in the diaminopimelate dehydrogenase dimer, as found in the monoclinic space group asymmetric unit, and the Cα trace of the monomer in the trigonal space group (binary complex, blue).

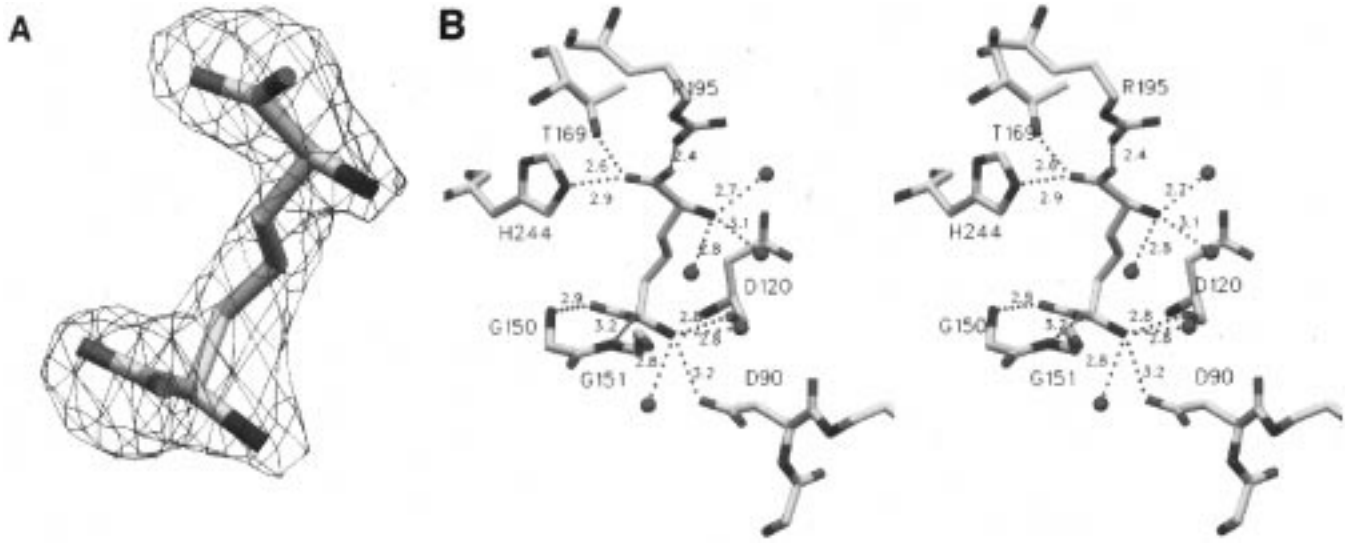

FIGURE 3: (A) Difference Fourier electron density map for the diaminopimelate dehydrogenase−DAP complex used to locate the bound substrate. The map was calculated at 2.8 Å and contoured at 2.5σ. (B) DAP binding site. All of the interactions made by the bound substrate with protein atoms are represented as dotted lines.

that while in the closed conformer both NADPH and substrate are inaccessible to solvent, in the open conformer the dinucleotide is completely accessible to solvent. However, in the intermediate conformation observed here, the bound DAP is surrounded by protein atoms, while the dinucleotide binding site is relatively open and would allow for cofactor binding. This structure, as well as hydrogen/deuterium exchange data (*23*) showing that the enzyme is capable of binding the *meso*-DAP in the absence of nucleotide, suggests that the *C. glutamicum* enzyme may exhibit a kinetic mechanism different from the ordered kinetic mechanism proposed for the *Bacillus* enzyme (*12*).

Diaminopimelic Acid Binding Site. Diaminopimelate dehydrogenase must distinguish between the L- and D-amino acid centers on the same symmetric molecule. The enzyme is highly specific for *meso*-DAP and for the *Bacillus* and *C. glutamicum* enzymes; both L,L- and D,D-DAP are competitive inhibitors versus *meso*-DAP, exhibiting millimolar K_i values (*7*, *8*, *12*). The structure of the binary diaminopimelate dehydrogenase−DAP complex provides some insights into the molecular basis of this stereospecificity. Analysis of a ($|F_o - F_c|\phi_c$) difference Fourier electron density map calculated for the enzyme−DAP complex after the first round of refinement clearly showed the presence of residual positive electron density in the area that had been previously proposed to be the substrate binding site (*16*). A molecule of *meso*-DAP was appropriately fitted into this density, with its D center closer to the dinucleotide binding domain and the three intervening carbon atoms separating the D and L centers in an almost *all-trans* conformation. This orientation of the substrate juxtaposes the α-hydrogen of the D-amino acid center transferred during catalysis toward the C4′ of the nicotinamide ring. Figure 3A shows the electron density into which *meso*-DAP was fitted, and Figure 3B is a stereoview of the interactions made between the substrate and protein atoms. The DAP binding site is an elongated cavity, bordered on three sides by main chain and side chain atoms of residues that belong to all three domains of the enzyme:

Asp90−His92 and Leu265−Pro271 from the dinucleotide binding domain, Gly118−Met122, Thr142−Ser149, and His244 from the dimerization domain, and Gln150−Gly151, Thr169, and Arg195 from the C-terminal amino acid-binding domain. The fourth side is solvent exposed, and several ordered water molecules have been refined in this area, as well as in the dinucleotide binding pocket. The methylene groups of bound DAP lie against the protein and are within van der Waals distance from the side chains of Trp119 and Asp120. The distal L center is stacked against the indole side chain of Trp144 (the two tryptophan residues are not shown for clarity in Figure 3B but are shown below in Figure 5B). Hydrogen-bonding interactions with protein atoms are predominantly made with the two carboxylate groups of *meso*-DAP, while the two amino groups interact with ordered solvent molecules. The distribution of hydrogen bond donors (i.e., main chain amide nitrogens, arginine, threonine, and histidine side chains) and hydrogen bond acceptors (i.e., main chain carbonyl oxygens, aspartate carboxylates, and solvent molecules) determines the orientation of the substrate. Thus, the carboxylic acids of *meso*-DAP face the side of the cavity bordered by protein atoms, while the amino groups of *meso*-DAP face the solvent-accessible side. These polar interactions constrain the *meso* substrate to a unique orientation for productive catalysis and define the stereochemical requirements for oxidation of the D-amino acid center. Attempts to position the L-amino acid center adjacent to the nucleotide in a conformation that would satisfy the hydrogen-bonding arrangement of the binding site residues would orient the Cα-hydrogen bond away from the nicotinamide ring, explaining the lack of activity with substrate analogues possessing an L center. Attempts to model a D,D-DAP molecule into this binding site made it clear that a distal L center is required in order to maintain the maximum number of favorable electrostatic and hydrophobic interactions at the distal site while maintaining the correct orientation at the catalytic site (results not shown). This hypothesis has been confirmed by the determination of the structure of a ternary diaminopimelate dehydrogenase−$NADP^+$−inhibitor complex described below.

Inhibitor Binding Site. Although few detailed mechanistic studies have appeared concerning diaminopimelate dehydrogenase, the detailed studies of the chemical mechanisms of related amino acid dehydrogenases have served as a template for inhibitor design. Thus, a reasonable chemical mechanism for the dehydrogenase would include reaction of ammonia with the acyclic form of L-tetrahydrodipicolinate, L-2-amino-6-oxopimelate, to generate the corresponding imine. Reduction of this imine by hydride transfer from NADPH to the *si* face of the imine would generate the product, *meso*-DAP (Scheme 3). Inhibitors which mimicked the bound imine intermediate would be expected to bind tightly to the dehydrogenase. In addition, the reaction which generates *meso*-DAP from L,L-DAP in the succinylase pathway, catalyzed by the *dap*F-encoded diaminopimelate epimerase (EC 5.1.1.7), would also be expected to involve an sp^2-hybridized intermediate in the epimerization reaction and be inhibited by compounds such as isoxazolines. The synthesis of such inhibitors has been reported, and in particular, the (2*S*,5*S*)-isoxazoline was shown to be a potent inhibitor of the *B. sphaericus* diaminopimelate dehydrogenase (*13*). The inhibition constant (K_i) for the reductive

Scheme 3

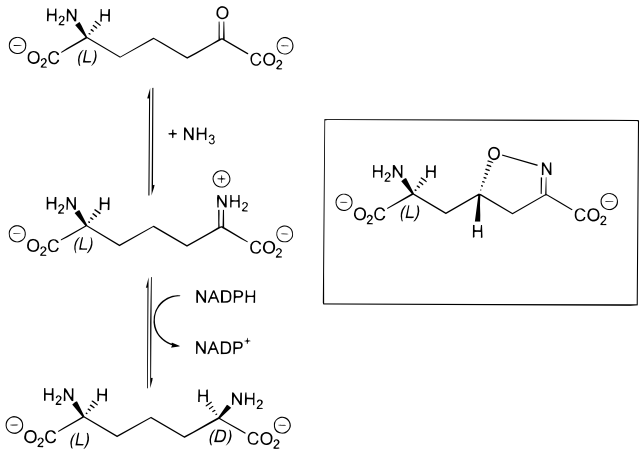

amination reaction was 4.2 μM, while the corresponding value for the oxidative deamination reaction was 23 μM at pH 7.8 (*13*). On the other hand, the isomeric (2*S*,5*R*)-isoxazoline does not display significant inhibition of the dehydrogenase reaction at millimolar concentrations. The *C. glutamicum* diaminopimelate dehydrogenase was crystallized in the presence of $NADP^+$ and the (2*S*,5*S*)-isoxazoline. A ($|F_o| - |F_c|)\phi_c$) difference Fourier electron density map, calculated at 2.2 Å resolution using the F_o from the ternary complex and F_c and phases from the protein model, clearly showed electron density corresponding to the presence of the bound inhibitor (Figure 4A). The electron density map is of sufficient quality to permit the inhibitor to be oriented unequivocally. Panels B and C of Figure 4 are representations of the interactions made by the inhibitor with protein and solvent atoms and an overlay of the inhibitor and DAP in the binding site, respectively. The inhibitor and DAP bind in equivalent positions, with the carboxylates of *meso*-DAP and the inhibitor being within 1.0 Å from each other. The interactions made between the inhibitor and enzyme main chain and side chain atoms are also very similar to those previously described for the substrate. The nitrogen and oxygen atoms of the isoxazoline ring are located in the solvent-exposed area of the binding site and make two hydrogen bond interactions with ordered solvent molecules. The remaining carbon atoms of the ring and the C4 methylene carbon connecting the L-amino acid center and isoxazoline ring are positioned within van der Waals distance of the side chain of Trp119, Trp144, and His 144. The L-amino acid center of the inhibitor occupies the same position as the D-amino acid center of bound *meso*-DAP, but being of opposite stereochemical configuration, its Cα−H bond points away from the C4 position of the nicotinamide ring of bound $NADP^+$. This orientation explains the lack of activity of the compound with the dehydrogenase and its inhibitory efficacy. Surprisingly, the orientation of the inhibitor is opposite to the one predicted in which the planar sp^2-hybridized carbon of the ring would be oriented proximal to the bound nucleotide and with the L-amino acid center superimposed on the corresponding L center of bound DAP. This expected orientation is shown in Figure 5A, along with the experimental electron density. With the inhibitor bound in this way, the aliphatic portion of the five-membered ring is exposed to the solvent, and the polar nitrogen and oxygen ring atoms are forced against protein atoms. Comparison

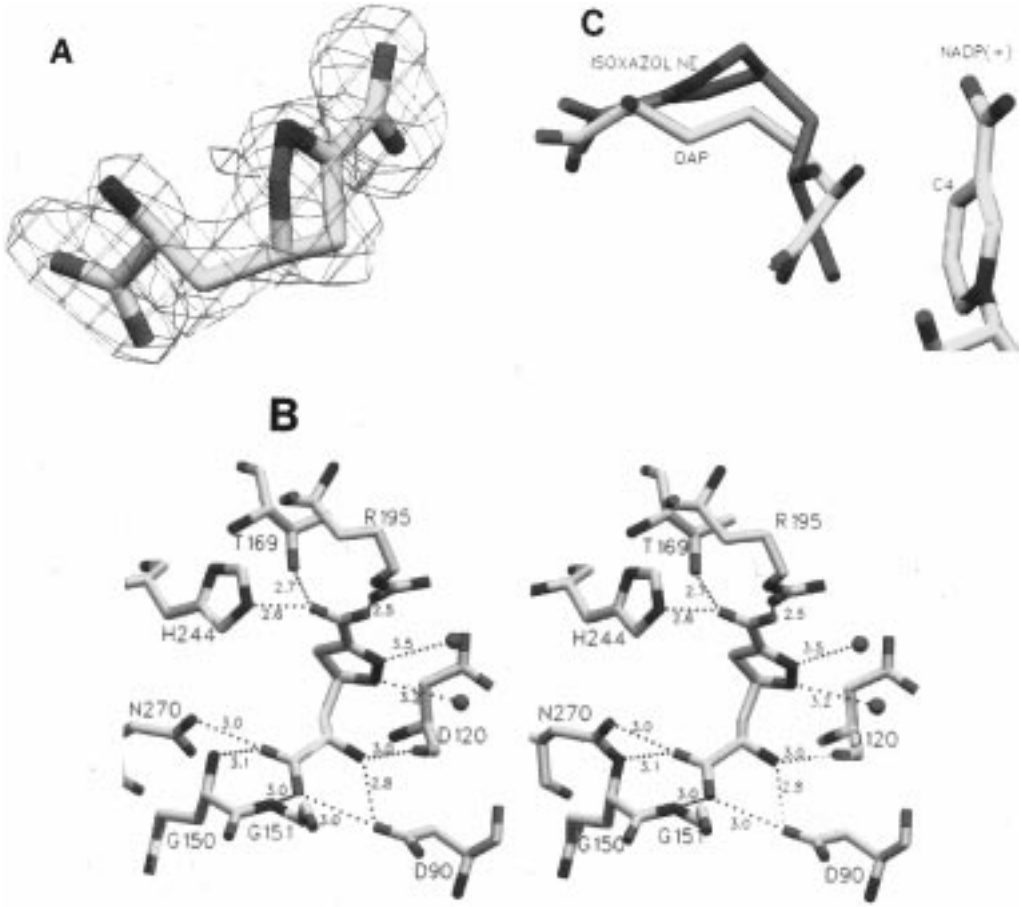

FIGURE 4: (A) Difference Fourier electron density map for the diaminopimelate dehydrogenase−$NADP^+$ inhibitor complex used to locate the bound isoxazoline. The map was calculated at 2.2 Å and contoured at 2.5σ. (B) Isoxazoline binding site. All of the interactions made by the bound substrate with protein atoms are represented as dotted lines. (C) Overlay of DAP and the inhibitor in the diaminopimelate dehydrogenase substrate binding site.

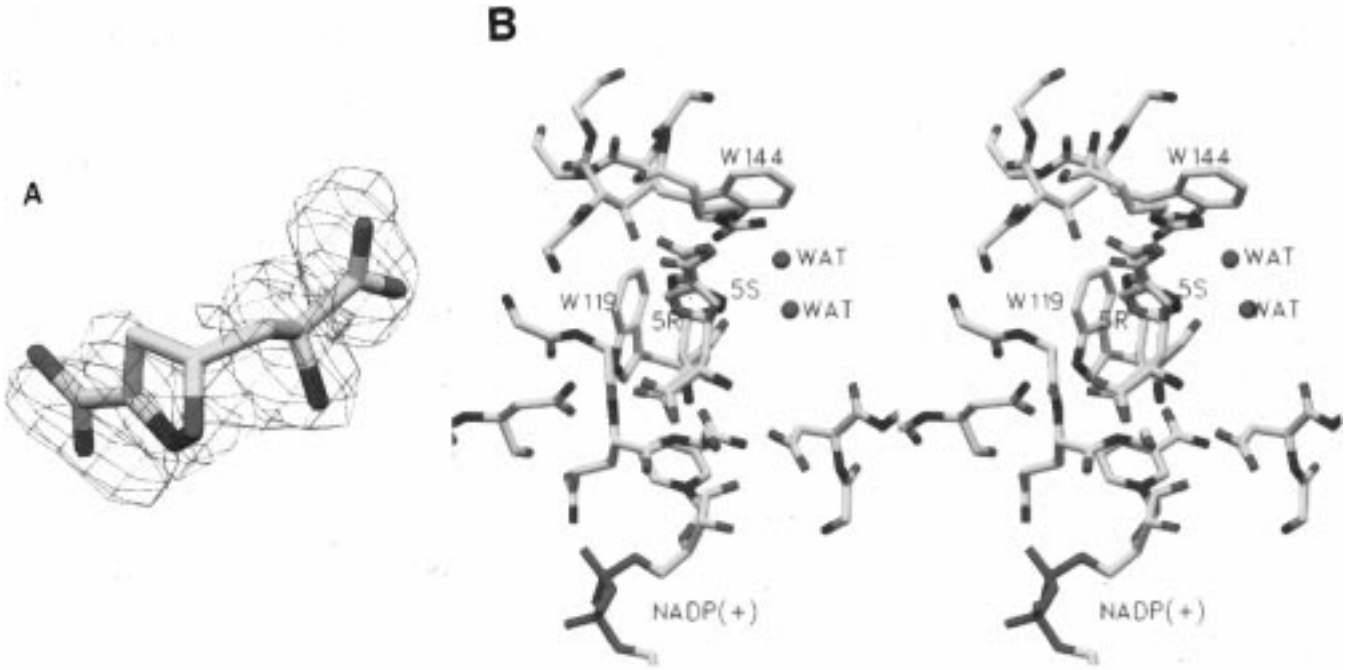

FIGURE 5: (A) Inhibitor modeled within the experimental electron density map in the dehydrogenase substrate binding site. (B) Overlay of the (2*S*,5*S*)- and (2*S*,5*R*)-isoxazoline stereoisomers in the substrate binding site.

of these two binding modes makes it clear that this second orientation would result in an overall loss of favorable interactions. Similar reasoning and model building provide an explanation for the much poorer inhibitory activity of the isomeric (2*S*,5*R*)-isoxazoline. A model of the 2*S*,5*R* isomer, built and docked into the binding site maintaining the

maximum number of interactions of the two carboxylates with the protein (Figure 5B), shows that the isoxazoline ring is in an orientation similar to that observed when the 2*S*,5*S* isomer is positioned with its L center superimposed on the L center of bound *meso*-DAP.

The present study demonstrates that rational design of enzyme inhibitors based on putative transition-state structures requires support from detailed structural analyses. Although direct superposition of half of the normal substrate, *meso*-DAP, on the potent inhibitory analogue, (2*S*,5*S*)-isoxazoline, is possible with coincidence of at least 14 atoms, crystallographic analysis shows that the actual binding occurs in the opposite orientation. Apparently, the isoxazoline moiety has a preference to occupy the distal, nonreactive, binding pocket for the L-amino acid center in the dehydrogenase, thus positioning the L-amino acid center of the inhibitor in the position occupied by the oxidizable D-amino acid center of *meso*-DAP. This binding mode also accounts for the potent competitive inhibition and limited antimicrobial activity against *B. sphaericus*, an organism that exclusively employs the DAP dehydrogenase pathway to synthesize *meso*-DAP and L-lysine (*13*).

REFERENCES

1. Cox, R. J. (1996) *Nat. Prod. Rep. 13*, 29−43.
2. Scapin, G. S., and Blanchard, J. S. (1997) *Adv. Enzymol. 72A*, 279−324.
3. Kindler, S. H., and Gilvarg, G. (1960) *J. Biol. Chem. 235*, 3532−3535.
4. Berges, D. A., DeWolf, W. E., Dunn, G. L., Newman, S. J., Schmidt, J., Taggart, J., and Gilvarg, G. (1986) *J. Biol. Chem. 261*, 6160−6167.
5. Sundharadas, G., and Gilvarg, G. (1967) *J. Biol. Chem. 242*, 3983−3988.
6. White, P. J. (1983) *J. Gen. Microbiol. 129*, 739−749.
7. Misono, H., Ogaswara, M., and Nagasaki, S. (1986a) *Agric. Biol. Chem. 50*, 1329−1330.
8. Misono, H., Ogaswara, M., and Nagasaki, S. (1986b) *Agric. Biol. Chem. 50*, 2729−2734.
9. Schrumpf, B., Schwarzer, A., Kalinowiski, J., Puhler, A., Eggeling, L., and Sahm, H. (1991) *J. Bacteriol. 173*, 4510−4516.
10. Sonntag, K., Eggeling, L., De Graaf, A. A., and Sahm, H. (1993) *Eur. J. Biochem. 213*, 1325−1331.
11. Brunhuber, N. M. W., and Blanchard, J. S. (1994) *Crit. Rev. Biochem. Mol. Biol. 29*, 415−467.
12. Misono, H., and Soda, K. (1980) *J. Biol. Chem. 255*, 10599−10605.
13. Abbot, S. D., Lane-Bell, P., Kanwar, P. S. S., and Vederas, J. C. (1994) *J. Am. Chem. Soc. 116*, 6513−6520.
14. Ishino, S., Mizukami, T., Yamaguchi, K., Katsumata, R., and Araki, K. (1987) *Nucleic Acids Res. 15*, 3917.
15. Reddy, S. G., Scapin, G., and Blanchard, J. S. (1996) *Proteins: Struct., Funct., Genet. 25*, 514−516.
16. Scapin, G. S., Reddy, S. G., and Blanchard, J. S. (1996) *Biochemistry 35*, 13540−13551.
17. Howard, A. J. (1986) *A guide to data reduction for the Nicolet Imaging Proportional Counter: the XENGEN system*, Protein Engineering Department, Genex Corp., 16020 Industrial Drive, Gaithersburg, MD 20877.
18. Mathews, B. W. (1968) *J. Mol. Biol. 33*, 491−492.
19. Navaza, J. (1994) *Acta Crystallogr. A50*, 157−163.
20. Brunger, A. T. (1992) *X-PLOR version 3.1 manual: a system for crystallography and NMR*, Yale University, New Haven, CT.
21. Roberts, A. L. U., and Brunger, A. T. (1995) *Acta Crystallogr. D51*, 990−1002.
22. Kleyvegt, G. T., and Brunger, A. T. (1996) *Structure 4*, 897−904.
23. Wang, F., Scapin, G., Blanchard, J. S., and Angeletti, R. H. (1998) *Protein Sci.* (in press).
24. Baker, P. J., Britton, K. L., K. S., Rice, D. W., Rob, A., and Stillman, T. J. (1992a) *J. Mol. Biol. 215*, 403−410.
25. Baker, P. J., Britton, K. L., Engel, P. C., Farrants, G. W., Lilley, K. S., Rice, D. W., and Stillman, T. J. (1992b) *Proteins: Struct., Funct., Genet. 12*, 75−86.
26. Stillman, T. J., Baker, P. J., Britton, K. L., and Rice, D. W. (1993) *J. Mol. Biol. 234*, 1131−1139.
27. Nicholls, A., Sharp, K., and Honig, B. (1991) *Proteins: Struct., Funct., Genet. 11*, 281.

BI9727949